Supramolecular Sequential Assembly of Polymer Thin Films Based on Dimeric, Dendrimeric, and Polymeric Schiff-Base Ligands and Metal Ions

ARTICLE *in* LANGMUIR · APRIL 2007

Impact Factor: 4.46 · DOI: 10.1021/la062044c · Source: PubMed

6 AUTHORS, INCLUDING:

Raman Rabindranath
Fraunhofer Institute for Silicate Research ISC
15 PUBLICATIONS **439** CITATIONS

Supramolecular Sequential Assembly of Polymer Thin Films Based on Dimeric, Dendrimeric, and Polymeric Schiff-Base Ligands and Metal Ions

Badreddine Belghoul, Irina Welterlich, Anna Maier, Ali Toutianoush, A. Raman Rabindranath, and Bernd Tieke*

Institut für Physikalische Chemie, der Universität zu Köln, Luxemburgerstr. 116, D-50939 Köln, Germany

Received July 14, 2006. In Final Form: January 30, 2007

New metal−Schiff-base coordination polymer films were prepared using multiple sequential adsorption of metal ions and salen-based ligand molecules. As the ligands, bis-bidentate 5,5′-methylene-bis(*N*-methylsalicylidenamine) (MBSA), tetra-bidentate *N*,*N*′,*N*″,*N*‴-tetrasalicylidene-polyamidoamine (TSPA), and multi-bidentate poly(*N*-salicylidenevinylamine) (PSVA) were used. The metal ions were Cu(II), Zn(II), Fe(II), Fe(III), and Ce(IV). The resulting films are deeply colored due to the formation of coordinative bonds between the metal ions and the salen groups. Our study indicates that film formation becomes progressively easier, if the number of salen groups per ligand molecule increases. While Cu(II), Ni(II), Fe, and Ce(IV) are well suited for complex formation, Zn(II) is less suited. Possible structures of the polymers are discussed. Cyclic voltammetric studies of the films are also presented.

1. Introduction

In recent years, transition metal coordination polymers have found increasing interest in macromolecular and supramolecular science because of their electronic, magnetic, optic, sensor, and catalytic properties.[1] Unfortunately, the polymers are often scarcely soluble and are difficult to process into thin films by common procedures. As recently demonstrated, layer-by-layer (lbl) assembly techniques provide a simple yet elegant means to prepare well-organized organic, organic−inorganic, and purely inorganic ultrathin films.[2] Lbl assembly is based on electrostatic interaction between cationic and anionic species,[2,3] hydrogen bonding,[4−6] hydrophobic interaction,[7] or coordinative bond formation between transition metal ions and organic ligands, with the latter also being called "reactive self-assembly".[8−10] Reactive self-assembly is especially attractive for the preparation of ultrathin films of supramolecular coordination polymers. Recent examples comprise new ultrathin films of zinc-bisquinoline,[11] zirconium-tetrasalicylidene-diaminobenzidine,[12] metal tetrathiooxalates,[13,14] and others,[15−17] which exhibit interesting photo- and electroactive properties.[13−15] A general reaction scheme describing the reactive self-assembly of bis-bidentate ligands and divalent metal ions under the formation of coordination polymer films is outlined in Figure 1.

Our present work is aimed at describing new ultrathin films of supramolecular coordination polymers using the approach of reactive self-assembling. As useful ligands, we have chosen molecules containing salicylideneamine ("salen") groups, which are known to react with transition metal ions to form stable metal−ligand complexes: bis-bidentate 5,5′-methylene-bis(*N*-methylsalicylideneamine) (MBSA), tetra-bidentate *N*,*N*′,*N*″,*N*‴-tetrasalicylidene-polyamidoamine (TSPA), and multi-bidentate poly(*N*-salicylidenevinylamine) (PSVA). The chemical structures are shown in Figure 2. As metal ions, Cu(II), Zn(II), Ni(II), Fe(II), Fe(III), and Ce(IV) were used.

First, we were interested in the question of whether a sequential buildup of organized polymer films is possible starting from simple bifunctional ligand molecules and various transition metal ions. Moreover, we wanted to answer the question of how the functionality of the ligand molecules and the valency of the metal ions affect the film formation. In previous studies, mainly bifunctional ligand molecules and divalent metal ions were used. In our study, bi-, tetra-, and polyfunctional salen-based compounds were used. In addition, we combined the ligands with di-, tri-, and tetravalent metal ions, which are known to form complexes of different geometries. Apart from a long chain derivative of MBSA, which was previously used for the preparation of Langmuir−Blodgett films of a Schiff-base coordination polymer,[18,19] the compounds used in our study as well as the corresponding supramolecular coordination polymers and the lbl assemblies have not been described yet. In our contribution, we report on the preparation of the monomers, the formation of the ultrathin films, and their characteristic optical and electrochemical properties using UV spectroscopy and cyclic voltammetry.

* To whom correspondence should be addressed.

(1) Rehahn, M. *Acta Polym.* **1998**, *49*, 201.
(2) *Multilayer Thin Films: Sequential Assembly of Nanocomposite Materials*; Decher, G., Schlenoff, J. B., Eds.; Wiley-VCH: Weinheim, 2003.
(3) Decher, G.; Hong, J. D. *Macromol. Symp.* **1991**, *46*, 321.
(4) Stockton, W. B.; Rubner, M. F. *Macromolecules* **1997**, *30*, 2717.
(5) Wang, L.; Wang, Z. Q.; Zhang, X.; Shen, J. C.; Chi, L. F.; Fuchs, H. *Macromol. Rapid Commun.* **1997**, *18*, 509.
(6) Wang, L.; Fu, Y.; Wang, Z.; Fan, Y.; Zhang, X. *Langmuir* **1999**, *15*, 1360.
(7) Serizawa, T.; Hashaguchi, S.; Akashi, M. *Langmuir* **1999**, *15*, 5363.
(8) Guang, C.; Hong, H.; Mallouk, T. E. *Acc. Chem. Res.* **1992**, *25*, 247.
(9) Hao, E.; Wang, L.; Zhang, J.; Yang, B.; Zhang, X.; Shen, J. *Chem. Lett.* **1999**, *28*, 5.
(10) Mwaura, K.; Thomsen, D. L.; Phely-Bobin, T.; Taher, M.; Theodoropulos, S.; Papadimitrakopoulos, F. *J. Am. Chem. Soc.* **2000**, *122*, 2647.
(11) Thomsen, D. L.; Phely-Bobin, T.; Papadimitrakopoulos, F. *J. Am. Chem. Soc.* **1998**, *120*, 6177.
(12) Byrd, H.; Holoway, C. E.; Poque, J. *Polym. Prepr. (Am. Chem. Soc., Div. Polym. Chem.)* **1997**, *38* (2), 167.
(13) Pyrasch, M.; Amirbeyki, D.; Tieke, B. *Adv. Mater.* **2001**, *13*, 1188.
(14) Pyrasch, M.; Amirbeyki, D.; Tieke, B. *Colloids Surf., A* **2002**, *198−200*, 425.
(15) Abe, M.; Michi, T.; Sato, A.; Kondo, T.; Zhou, W.; Ye, S.; Uosaki, K.; Sasaki, Y. *Angew. Chem., Int. Ed.* **2003**, *42*, 2912.
(16) Wanunu, M.; Vaskevich, A.; Cohen, S. R.; Cohen, H.; Arad-Yelin, R.; Shanzer, A.; Rubinstein, I. *J. Am. Chem. Soc.* **2005**, *127*, 17877.
(17) Evans, S. D.; Ulman, A.; Goppert-Berarducci, K. E.; Gerenser, L. J. *J. Am. Chem. Soc.* **1991**, *113*, 5866.
(18) Wilde, J. N.; Wigman, A. J.; Nagel, J.; Oertel, U.; Beeby, A.; Tanner, B.; Petty, M. C. *Acta Polym.* **1998**, *49*, 294.
(19) Oertel, U.; Nagel, J. *Thin Solid Films* **1996**, *284−285*, 313.

10.1021/la062044c CCC: $37.00
Published on Web 03/31/2007

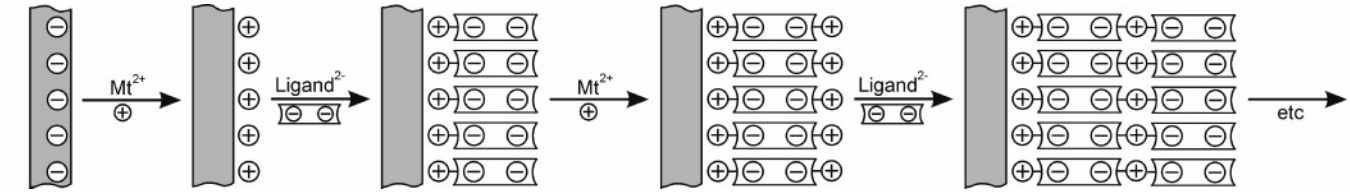

Figure 1. General scheme of the reactive self-assembly of divalent metal ions and bis-bidentate ligand molecules.

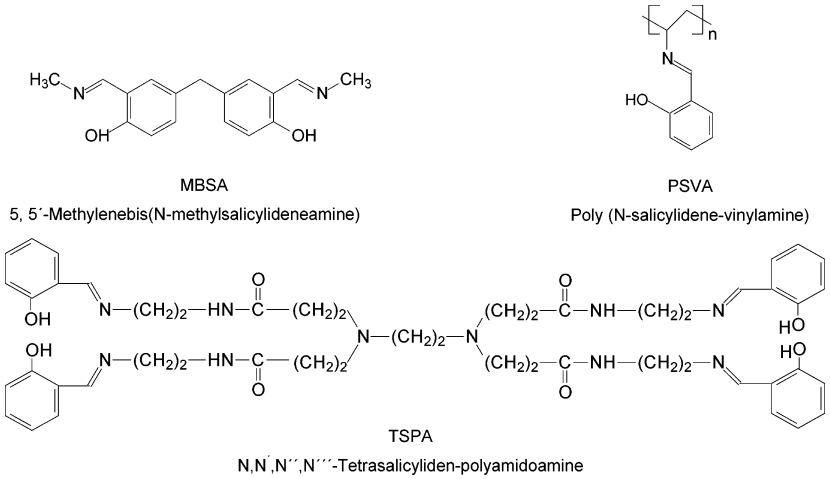

Figure 2. Chemical structures of Schiff-base ligands used in this study.

2. Experimental Section

2.1. Materials. Salicylaldehyde, trioxane, and polyamidoamine (PAMAM, 0. generation) were purchased from Fluka, Merck, and Aldrich and used without further purification. Polyvinylamine (PVA, MW 100 000) was kindly supplied by BASF AG, Ludwigshafen. Polyvinylsulfate potassium salt (PVS, MW 350 000) was obtained from Acros. $CuCl_2 \cdot 2H_2O$, $NiCl_2 \cdot 6H_2O$, $FeCl_2 \cdot 4H_2O$, $FeCl_3 \cdot 6H_2O$, and $(NH_4)_2Ce(NO_3)_6$ were obtained from Merck, Fluka, and Acros (analytical grade) and used without further purification. Ethanol p.a. was used as solvent for the buildup of the coordination polymer films.

2.1.1. Preparation of MBSA. In a two-necked flask equipped with a reflux condenser and dropping funnel, 3.75 mL (0.028 mol) of an ethanolic solution of methylamine (33 wt %) was mixed with 30 mL of ethanol p.a. and then the mixture was heated to 78 °C. A solution of 3.83 g (0.014 mol) of 5,5′-methylene bissalicylaldehyde[20] in 30 mL of ethanol was filled in the dropping funnel and then slowly added to the boiling methylamine solution. After boiling and stirring for 30 min, the mixture was cooled to room temperature. A yellow precipitate formed, which was filtered off and recrystallized from ethanol. Yield: 3.57 g (0.012 mol, 85%), mp 151 °C.

^{1}H NMR (toluene-d_8): δ (ppm) = 3.05 (d, 6H, 2 × CH_3), 3.8 (s, 2H, CH_2), 7.25 (m, 6H, arom.), 8.3 (s, 2H, 2 × CH), 13.2 (s, 2H, 2 × OH) (see also Figure 3a). UV (ethanol): 412, 326, 254, 228 nm.

2.1.2. Preparation of TSPA. In a three-necked flask equipped with a stirrer, reflux condenser, and dropping funnel, 4.13 g (8 mmol) of PAMAM (0. generation) was dissolved in 40 mL of dry ethanol. To the stirred solution, 4 g (33 mmol) of salicylaldehyde was added. The mixture was heated at 70 °C under nitrogen atmosphere for 2 h. After cooling to room temperature and standing overnight, a yellow precipitate was formed, which was filtered off, washed, and then dried in vacuum. Yield: 2.5 g (2.7 mmol, 33.7%), mp 148 °C.

^{1}H NMR ($CDCl_3$): δ (ppm) = 2.24 (t, 8H, 4 × CH_2), 2.34 (s, 4H, 2 × CH_2), 2.57 (t, 8H, 4 × CH_2), 3.51 (q, 8H, 4 × CH_2), 3.69 (t, 8H, 4 × CH_2), 6.9, 7.21, 7.24, 7.32 (m, 16H, arom.), 8.3 (d, 4H, 4 × CHN), 13.2 (s, 4H, 4 × OH) (see also Figure 3b). UV (ethanol): 411 nm, 317 nm (ϵ: 11.49 × 10^6 cm^2 mol^{-1}), 255 nm (34.53 × 10^6 cm^2 mol^{-1}), 214 nm (77.21 × 10^6 cm^2 mol^{-1}) (see also Figure 4a).

2.1.3. Preparation of PSVA. In a three-necked flask equipped with a stirrer, reflux condenser, and dropping funnel, 0.57 g (13.6 milli-monomol) of PVA was dissolved in 40 mL of dry ethanol. To the stirred solution, 4 g (33 mmol) of salicylaldehyde was added. The reaction mixture was heated at 70 °C under nitrogen atmosphere for 2 h. A yellow precipitate occurred, which was filtered, washed with ethanol, and then dried in vacuum. Yield: 0.3 g (2.0 mmol, 15%). Upon heating, the polymer changed from a yellow powder to a viscous liquid at 175 ± 2 °C.

^{1}H NMR (DMSO-d_6) (Figure 2): δ (ppm) = 1.7 (s, 2H, 1 × CH_2), 3.0 (s, 1H, 1 × CH), 6.6−7.1 (m, 4H, arom.), 8.0 (s, 1H, CHN), 13.0 (s, 1H, OH) (see also Figure 3c). UV (chloroform): 321 nm (ϵ: 3.127 × 10^6 cm^2 mol^{-1}), 259 nm (7.046 × 10^6 cm^2 mol^{-1}) (see also Figure 4b).

2.2. Precoating of Substrates. Quartz supports (Suprasil 30 × 12 × 1 mm^3, Hellma GmbH, Müllheim/Baden, Germany) and glass supports coated with a thin layer of indium−tin oxide (ITO, Plano, Wetzlar, resistance 100 Ω cm^{-2}) were used for the experiments. The quartz supports were cleaned in a 7:3 mixture of H_2SO_4/H_2O_2 (***Caution!*** *The mixture is strongly oxidizing and may detonate upon contact with organic material.*), washed with Milli-Q water, and subjected to ultrasonication in alkaline isopropanol and 0.1 M aqueous hydrochloric acid at 60 °C for 1 h each. After careful washing with Milli-Q water, the supports were silanized with 3-aminopropylmethyldiethoxysilane (Fluka) and then subsequently coated with one layer each of PVS, PVA, and PVS, as previously described.[21] ITO-coated glass supports were cleaned upon successive ultrasonication in ethanol and water at 60 °C for 30 min each. Ultrasonication was repeated three times. Then a layer of polydiallyldimethylammonium chloride (PDDA, MW 250 000) and a layer of PVS were deposited using the same dipping method as described for the quartz substrates.

2.3. Preparation of Polymer Films. For the buildup of the coordination polymer films, the pretreated substrates were successively dipped into (a) an ethanolic solution of the inorganic salt (concentration: 0.0015 mol/L), (b) pure ethanol, (c) an ethanolic solution of MBSA or TSPA (concentration: 0.0015 mol/L) or a chloroform solution of PSVA (concentration: 0.0015 mol/L), (d) pure ethanol, and so forth. Immersion times were 10 min each for steps (a) and (c) and 1 min each for steps (b) and (d). After steps (b) and (d), the substrates were dried in air for 5−10 min.

(20) Marvell, C. S.; Tarköy, N. *J. Am. Chem. Soc.* **1957**, *79*, 6000.

(21) Pyrasch, M.; Tieke, B. *Langmuir* **2001**, *17*, 7706.

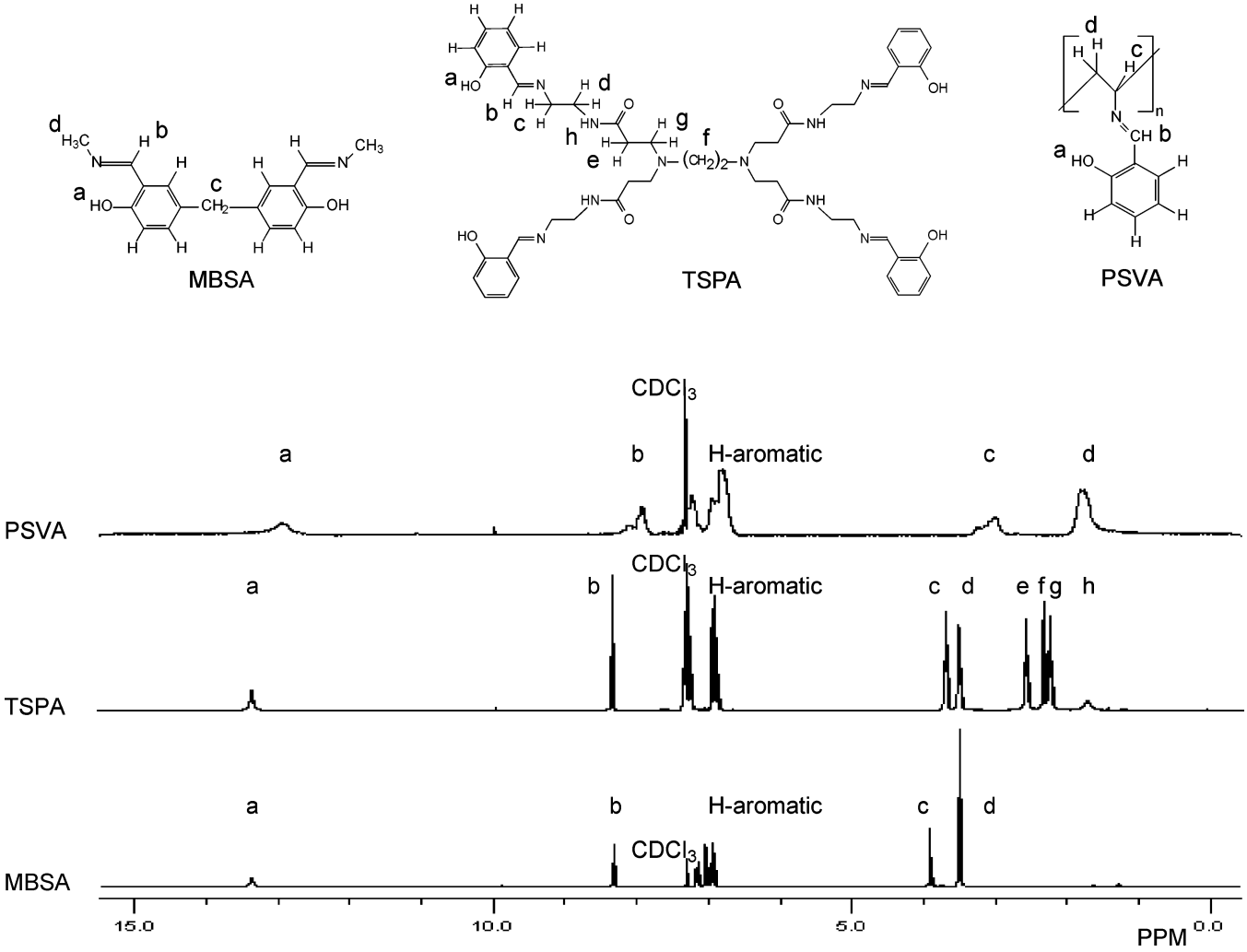

Figure 3. ^{1}H NMR spectra of ligand molecules used in this study: MBSA, TSPA, and PSVA.

Scheme 1. Scheme of the Formation of Mt(II)−MBSA Coordination Polymers

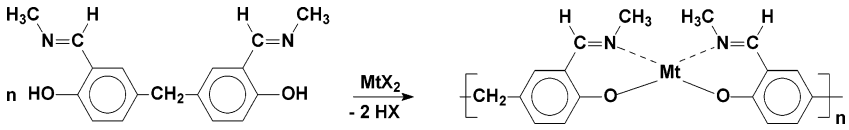

2.4. Methods. UV−visible absorption spectra were recorded using a Perkin-Elmer Lambda 14 spectrometer. All spectra were corrected by subtracting the signal of the pure quartz substrate. ^{1}H NMR spectroscopy was carried out using a 300 MHz-Bruker AC 300 spectrometer. Tetramethylsilane was used as the standard. Cyclic voltammetry was performed on a Heka potentiostat/galvanostat (model PG 390, Heka Electronic, Lambrecht, Germany). Data acquisition and potentiostat control were accomplished using the POTPULSE software, version 8.4 (Heka). All experiments were carried out in a 100 mL three-electrode glass cell at room temperature employing the polymer film on an ITO-coated glass substrate, a platinum wire as the reference electrode, and a platinum plate (4 cm^2) as the counter electrode. The electrochemical experiments were carried out in 0.5 M aqueous KCl solution (pH 5.5) or in acetonitrile containing 0.1 M tetrabutylammonium hexafluorophosphate, saturated with N_2. Cyclic voltammetric curves were recorded in the potential range from −0.8 to +1.2 V, and the scan rate was 3.5 or 20 mV/s. Scanning force microscopic (SFM) images were taken with a Nanoscope IV SFM (Digital Instruments) working in the contact mode. Self-assembled films on quartz slides were investigated in air at room temperature. Commercially available Si/N cantilevers with integrated tips were used. SEM images were measured using a Zeiss Supra 40 VP scanning electron microscope (detector: SE2, potential 1.0 kV). Self-assembled films on ITO-coated glass were investigated. Film thickness was measured with a Dektak 3 apparatus from Vecco. The film was partially scratched from the surface, and a height profile of the surface was scanned. The error in the measurements was ∼5 nm.

3. Results and Discussion

The Schiff-base ligand MBSA is easily accessible upon reaction of 5,5′-methylenebissalicylaldehyde with methylamine. The other ligands TSPA and PSVA are obtained upon reaction of the PAMAM dendrimer (0. generation) and polyvinylamine with salicylaldehyde, respectively. All compounds are yellow solids. MBSA and TSPA are well soluble in ethanol and dimethyl sulfoxide (DMSO), while PSVA is soluble in chloroform and DMSO. The proton NMR spectra of the ligands are shown in Figure 3. Because of its polymeric nature, PSVA exhibits rather broad signals. All spectra show the signal of the phenolic hydrogen at ∼13.2 ppm, the signal of the imine hydrogen at 8.0−8.3 ppm, and the signals of the aromatic groups at 6.6−7.3 ppm. The residual signals at 1.7−3.7 ppm can be ascribed to methylene H atoms and to the amide hydrogen atom in TSPA. The integral peak intensities are in good agreement with the chemical formulas, which are also displayed in Figure 3. The UV spectrum of TSPA

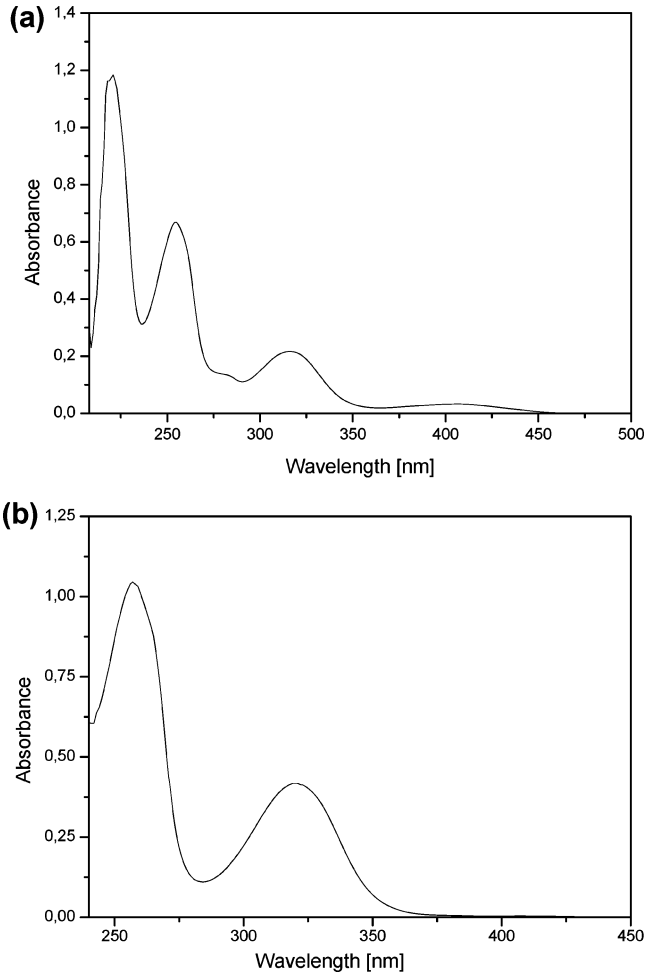

Figure 4. UV−visible spectra of TSPA in ethanol (a) and PSVA in chloroform (b).

in ethanol shows absorption maxima at 411, 317, 255, and 214 nm originating from the salen chromophor (Figure 4a). For MBSA, a similar spectrum with maxima at 412, 326, 254, and 228 nm is obtained, because this compound contains the same salen chromophor. The UV spectrum of PSVA in chloroform exhibits two strong bands at 321 and 259 nm, which again originate from the salen chromophor. The weak, long-wavelength band at ∼410 nm observed for TSPA and MBSA is missing (Figure 4b), perhaps due to the use of another solvent. Addition of transition metal salts led to a color change of the ligand solution due to the formation of the coordination polymers. For example, the Cu−MBSA polymer in ethanol exhibits absorption maxima at 372, 272, and 228 nm. The coordination polymer slowly precipitated from solution.

3.1. Metal−MBSA Films. Films of metal−MBSA coordination polymers were prepared on pretreated quartz substrates as described in the Experimental Section. At first, the substrates were dipped into the ethanolic solution of a divalent transition metal salt. The metal ions were adsorbed at the substrate surface, and the surface charge was reverted. After removing excess metal ions upon immersion in pure ethanol, the substrate was dipped into the ethanolic solution of MBSA, and the ligand molecules were adsorbed due to salt formation of the metal ions with the phenolic OH-groups and coordination with the N atoms of the aldimine groups. After removing excess ligand molecules upon immersion in ethanol, the substrate was dipped in the solution of the metal salt again, and so forth. After repeated dipping, a linear coordination polymer is formed on the substrate as indicated

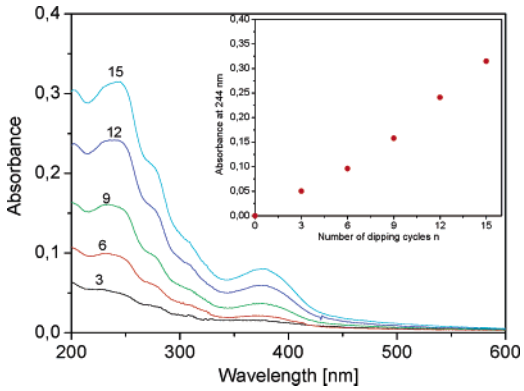

Figure 5. UV−visible spectra of Cu−MBSA films prepared upon multiple sequential adsorption. The inset indicates an increase of the absorption at 244 nm with the number of dipping cycles.

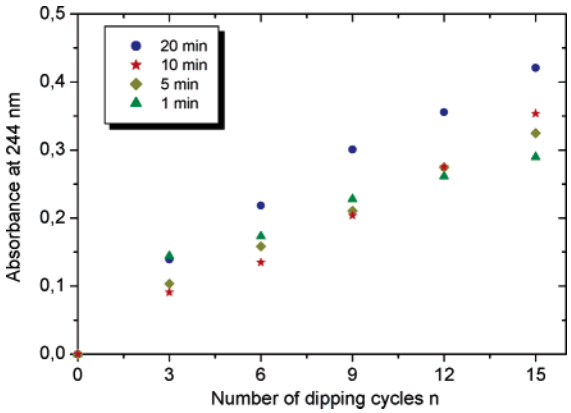

Figure 6. Plot of the absorbance of Cu−MBSA films at 244 nm versus the number of dipping cycles. Individual films were immersed in the dipping solutions for different time periods.

in Scheme 1. The amount of deposited material and the film thickness are controlled by the number of dipping cycles applied. Due to the deposition of the polymer, a gradual yellowish to brownish coloration of the substrates became obvious. It should be noted that only alternate dipping into the solutions of the metal salts and the ligand molecules led to film formation, while repeated dipping into only one of the two solutions did not lead to further adsorption of material.

In Figure 5, UV−visible spectra of films of the Cu−MBSA coordination polymer are shown, which were prepared with different numbers of dipping cycles. Due to the complex formation with Cu, the spectra differ from the solution spectrum of MBSA but resemble the solution spectrum after the addition of copper(II) chloride. The absorption maxima occur at 377 and 244 nm, and a shoulder occurs at 270 nm. This can be taken as proof for the formation of the coordination polymer on the substrate. As shown in the inset of Figure 5, the absorption increases almost linearly with the number of dipping cycles. This indicates that almost the same amount of polymer was adsorbed in each dipping cycle.

To optimize film growth, the dipping time and the concentration of the dipping solutions were varied. In Figure 6, the 244 nm absorption of films immersed in the dipping solutions for different time periods is plotted versus the number of dipping cycles. For all samples, the absorption increases with the number of dipping cycles, but remarkable differences are apparent for samples dipped either briefly or for a long time. At short dipping times, an initial strong increase in the absorption is found, which only slightly increases upon further dipping. If the dipping time is longer, the film growth becomes more linear. An optimum linear growth is

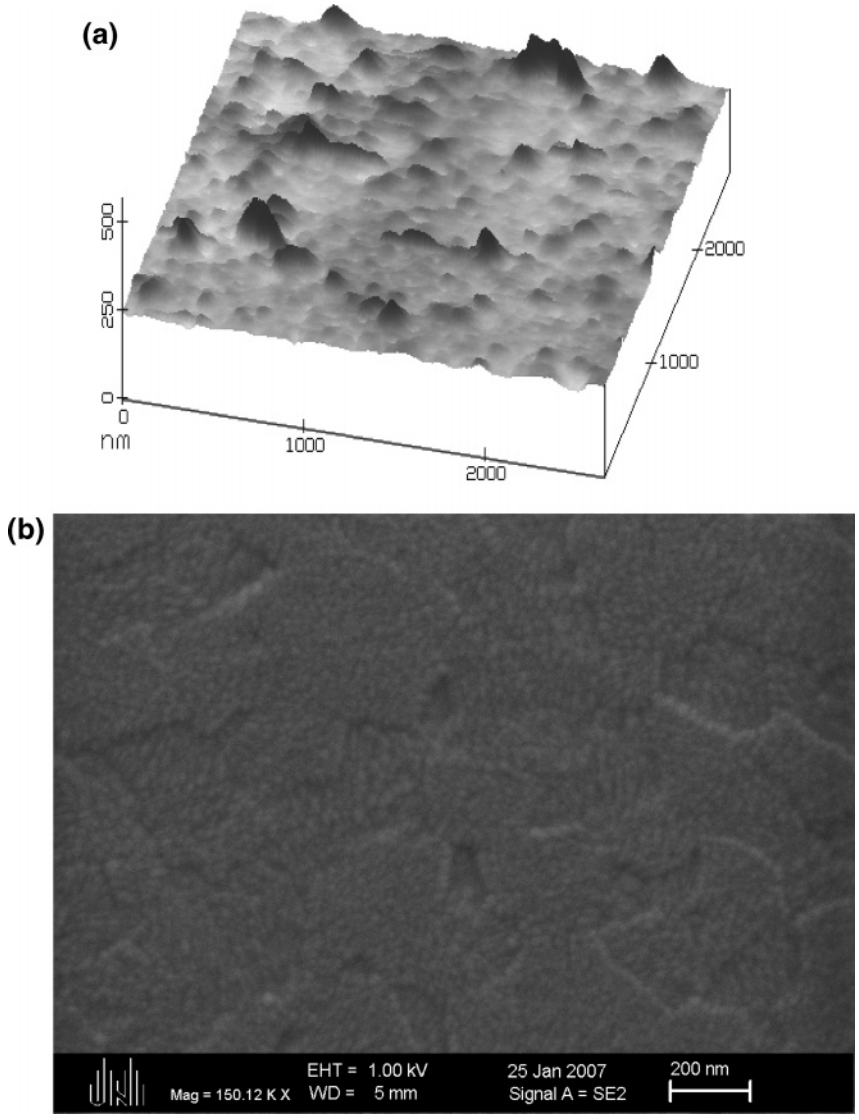

Figure 7. (a) SFM picture of a Cu−MBSA film (18 dipping cycles). The scan area is 2.7 μm × 2.7 μm. (b) SEM picture of a Cu−TSPA film (12 dipping cycles).

Scheme 2. Scheme of the Formation of Mt−TSPA Coordination Polymers

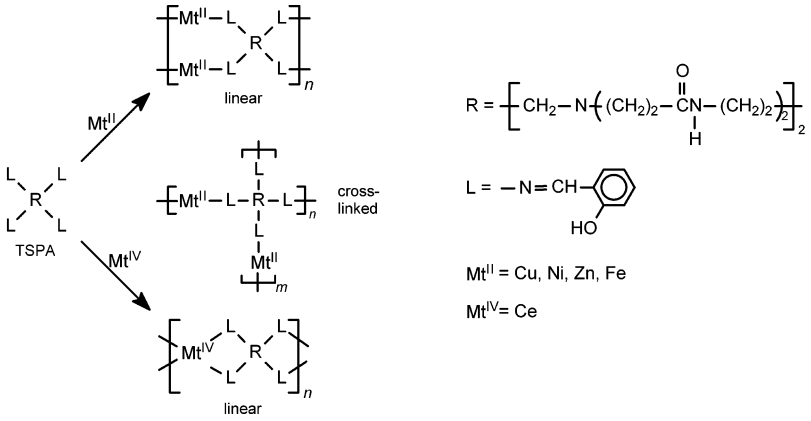

reached at a dipping time of 10 min. If the dipping time is 20 min, the film growth is only linear at a higher number of dipping cycles. For the first three dipping cycles, a stronger increase is found than for the subsequent ones. If the concentration of the dipping solution is changed, the amount of adsorbed material is also changed. While an exponential growth is found at concentrations up to 1×10^{-3} mol/L, the growth becomes linear when the concentration is increased to 1.5×10^{-3} mol/L. In all further experiments, the dipping time was 10 min and the concentration of the dipping solutions was always 1.5×10^{-3} mol/L.

Using these conditions, it was also possible to prepare coordination polymer films of MBSA and Ni(II), Fe(II), and Co(II), while attempts to prepare films with Zn(II) were only somewhat successful. The reason might be that Cu(II) and Ni(II) form square planar complexes and Fe(II) forms an octahedral

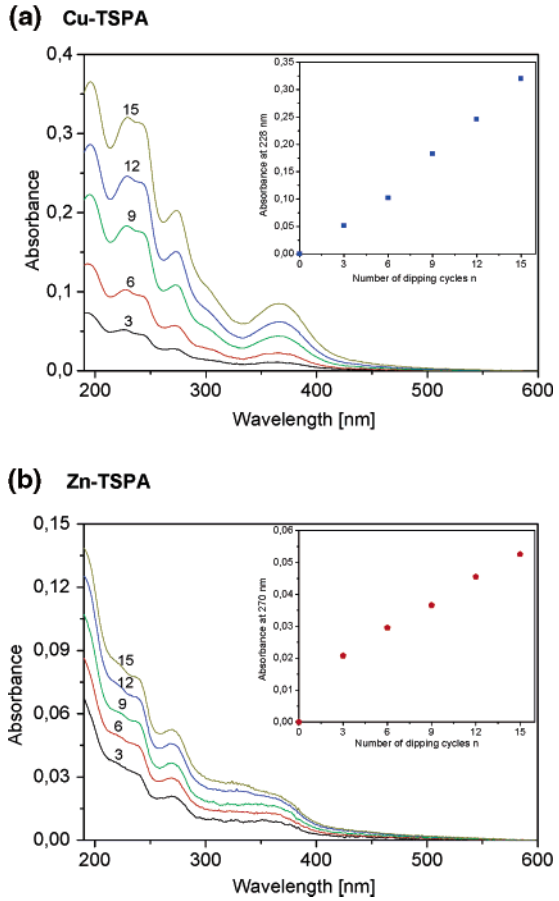

Figure 8. UV−visible spectra of metal−TSPA films prepared upon multiple sequential adsorption, with the metal ions being Cu(II) (a) and Zn(II) (b). The insets show an increase of the maximum absorbance with the number of dipping cycles.

complex, both of which are sterically favored geometries, whereas the tetragonal Zn(II) complexes are more voluminous and are therefore less likely to be formed in the densely packed thin films.

The surface of the Cu−MBSA films was characterized using scanning force and scanning electron microscopy. In Figure 7a, an SFM picture of a Cu−MBSA film prepared upon 18 dipping cycles is shown. The surface view of an area of 2.7 × 2.7 μm^2 indicates a rather smooth surface in which a few aggregates of up to 50 nm in height are embedded. The picture resembles the surface of poly(metal tetrathiooxalate) films.[15] It suggests that two growth mechanisms are involved in the film formation: one leading to a rather homogeneous surface deposition and the other leading to clustering and the formation of three-dimensional aggregates. In Figure 7b, an SEM picture of a Cu−TSPA film prepared upon 12 dipping cycles is shown. The surface view of an area of approximately 2 × 1.36 μm^2 again indicates a rather smooth surface with some small height differences. Films of Cu−PSVA show a similar surface structure. Profilometric studies of Cu−TSPA films (12 dipping cycles) and Cu−PSVA films (12 dipping cycles) indicate thicknesses of 10 ± 5 and 19 ± 5 nm, respectively. The larger thickness of the PSVA-containing sample indicates that the polymer is adsorbed in a coiled rather than in a flat conformation.

3.2. Metal−TSPA Films. Ultrathin films of metal−TSPA coordination polymers were prepared according to the same procedure as described above for the metal−MBSA films. If divalent transition metal ions such as Cu(II) and Ni(II) are used, the formation of square planar complexes is likely. As a consequence of the complex formation, either ladder-type linear polymers are formed or cross-linking may occur as outlined in Scheme 2. In Figure 8a, UV−visible spectra of Cu−TSPA films subjected to different numbers of dipping cycles are shown. The

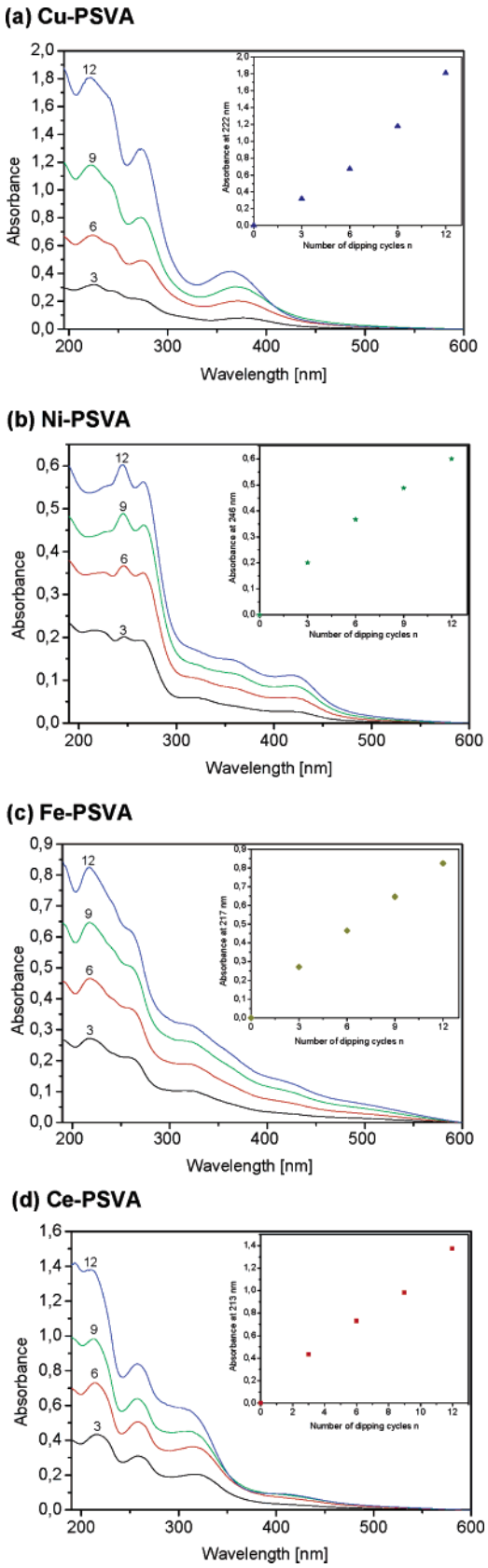

Figure 9. UV−visible spectra of metal PSVA−films prepared upon multiple sequential adsorption, with the metal ions being Cu(II) (a), Ni(II) (b), Fe(III) (c), and Ce(IV) (d).

Scheme 3. Scheme of the Formation of Mt(II)−PSVA Coordination Polymers

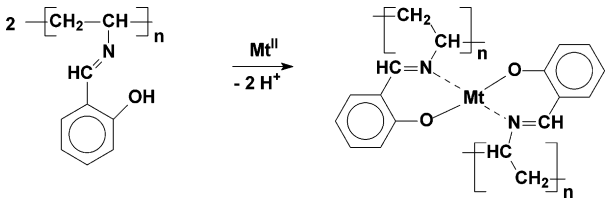

Scheme 4. Scheme of the Formation of Cross-Linked Ce(IV)−PSVA Coordination Polymers

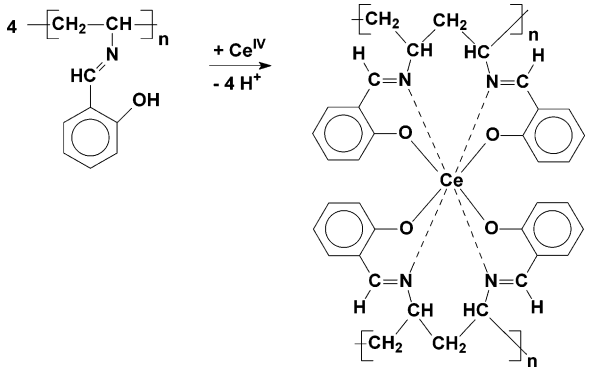

spectra resemble those of the Cu−MBSA films. Absorption maxima occur at 366, 273, 244, and 228 nm, and a further peak at 200 nm is apparent. The absorbance increases linearly with the number of dipping cycles applied, indicating regular film growth. Moreover, the increase of the absorbance per dipping cycle is the same as that for the Cu−MBSA films. This indicates the same chromophor density at the substrate surface. With TSPA, it was possible to prepare films of a Zn−TSPA coordination polymer. As indicated in the UV−visible spectra of Figure 8b, the films only exhibit a weak absorption with maxima at 270 and 236 nm and a shoulder at 357 nm. It is probably the more flexible molecular structure of TSPA which favors the formation of the metal complexes. In TSPA, four salen groups are present, which are linked to the molecule via flexible spacers, whereas MBSA only consists of two salen groups, which are bound together via a methylene group. Therefore, the more bulky tetrahedral structure of the Zn−salen complex can be formed more easily with TSPA.

It was also possible to build up coordination polymer films with Fe(II), Fe(III), and Ce(IV) ions (not shown). While the metal complex in the Ce(IV)−TSPA films probably exhibits an icosahedral structure, the corresponding complex in the Fe(III)−TSPA films is likely octahedral. The structure of the cerium complex is probably analogous to the recently reported structures of the metal−Schiff-base coordination polymers of Ce(IV) or Zr(IV) and *N*,*N*′,*N*″,*N*‴-tetrasalicylidene-3,3′-diaminobenzidine. As outlined in Scheme 2, the Ce(IV) ion is complexed by four salen groups originating from two TSPA molecules. As a result, a linear polymer is obtained.

3.3. Metal−PSVA Films. Films of the metal−PSVA complexes were prepared according to the same procedure as described for the metal−MBSA films. In Figure 9a, UV−visible spectra of Cu−PSVA films are shown, which were subjected to different numbers of dipping cycles. The spectra exhibit absorption maxima at 369, 273, and 222 nm and a shoulder at 248 nm. The high absorbance is striking. It is 10 times higher than those for the Cu−MBSA and Cu−TSPA films, which were prepared by the same number of dipping cycles. The reason is that the large number of Schiff-base binding sites attached to the polymer chains favors the adsorption and hinders the desorption of the

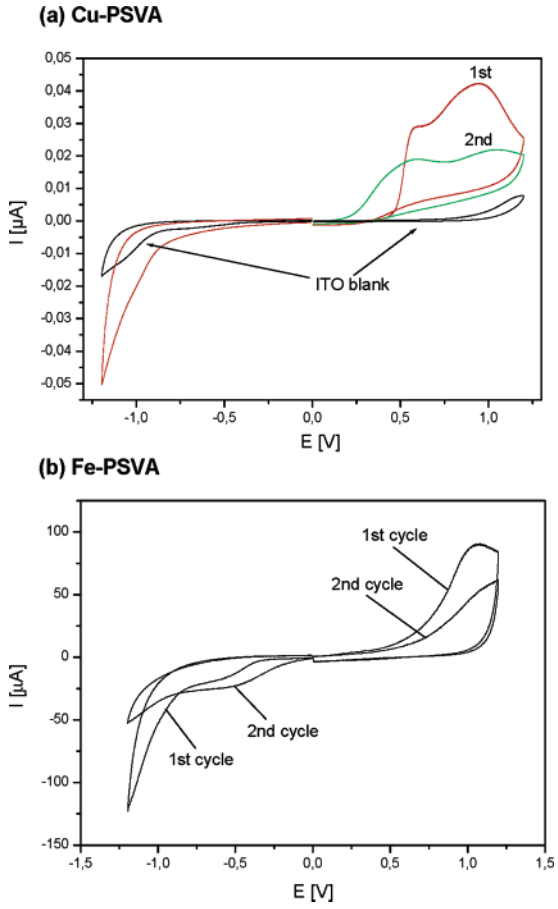

Figure 10. Cyclic voltammograms of films of Cu(II)−PSVA (a) and Fe(III)−PSVA (b) on ITO-coated glass electrodes (reference Pt). Measurements were carried out in a 0.1 M solution of tetrabutylammonium hexafluorophosphate in CH_3CN. Scan rates were (a) 20 and (b) 3.5 mV s^{-1}; T = 20 °C. In (a), the cyclic voltammogram of a blank ITO substrate is also shown. For further details, see text.

individual chains from the surface. Moreover, the adsorption of the polymeric ligands provides a much higher density of salen groups at the substrate surface than can be reached with any of the low molecular weight ligands. While the film growth of Cu−PSVA is slightly exponential (see the inset of Figure 9a), linear growth is found for Ni−PSVA, Fe(III)−PSVA, and Ce(IV)−PSVA. UV−vis spectra of Ni−PSVA coordination polymer films are shown in Figure 9b. Three absorption maxima at 422, 275, and 246 nm are apparent. The steady growth of the Cu- and Ni-based films may be favored by the formation of the square planar complexes of the metal ions with the salen units. In Scheme 3, the complex formation is described. If the complex is formed with two salen groups attached to different polymer chains, a highly cross-linked structure is obtained.

UV−visible spectra of the Fe(III)−PSVA and Ce−PSVA films are shown in Figure 9c and d. Films with Fe(III) as the metal ion exhibit absorption maxima at 322, 258, and 217 nm, and the spectrum exhibits a tail ranging up to 550 nm. Films with Ce(IV) ions exhibit a shoulder at 420 nm and show pronounced maxima at 325, 270, and 220 nm. While an octahedral coordination is likely for Fe(III), the Ce-containing films presumably exhibit the icosahedral coordination discussed above for the Ce−TSPA films. In Scheme 4, the formation of the polymeric Ce(IV)−Schiff-base complex is outlined. In this complex, four salen units are coordinated with one Ce(IV) ion. For steric reasons, it is likely that two salen units in neighboring positions at the polymer backbone always take part in the complex formation. The model

indicates that the Ce−PSVA coordination polymer films are also highly cross-linked.

3.4. Cyclovoltammetric Studies. To study the electrochemical behavior of the self-assembled films, the coordination polymers were deposited on ITO-coated glass plates. Films of the Cu(II)−PSVA, Fe(III)−PSVA, and Ce(IV)−PSVA coordination polymers were investigated using cyclic voltammetry. In Figure 10a, the voltammogram of the Cu(II)−PSVA film (six bilayers) cycled between −1.25 and +1.20 V versus Pt is shown. In the first cycle, two peak potentials at 0.6 and 0.9 V occur, indicating an oxidation of the Cu−PSVA film. In the subsequent reduction, no clear peak is apparent. However, in the second oxidative cycle, the same peak potentials as in the first run are found although the peaks are less intense and broadened. This indicates that the film was only partially restored after the first cycle; that is, the redox behavior is only partially reversible. In the subsequent oxidative cycles, the peak intensities further dropped, indicating a gradual decomposition (not shown). In the reductive cycle, no peaks can be found, indicating that the film is electrochemically inactive. For comparison, the voltammogram of a blank ITO substrate is also shown in Figure 10a.

The cyclic voltammetry diagram of the Fe(III)−PSVA film (12 bilayers) is shown in Figure 10b. The first oxidative cycle is accompanied by a single peak at ∼1 V. It is highly irreversible and can probably be ascribed to an oxidation of the ligand molecules. Upon subsequent reduction, a broad peak occurs at ∼ −0.6 V, which is also irreversible. Within the potential range investigated, any peak that could be related to the Fe(II)/Fe(III) couple is clearly missing. A similar electrochemical behavior was found for the Ce(IV)−PSVA films (not shown). Our studies do not indicate a reversible redox behavior in any of the investigated coordination polymer films.

4. Summary and Conclusions

Our study indicates that multiple sequential adsorption of bi- or multifunctional salen-based ligand molecules and numerous transition metal ions is a useful method for the preparation of ultrathin organized films of Schiff-base coordination polymers on solid supports. Among the ligand molecules used in our study, the polymeric ligands with many salen substituent groups turned out to be the most suited for this purpose. In general, the usefulness increased with the number of salen groups per molecule, simply because the adsorption of the highly functionalized molecules provides a higher density of reactive groups at the interface.

The best film formation is found for divalent transition metal ions such as Cu^{2+} and Ni^{2+}, which are able to form square planar Schiff-base complexes. However, other metal ions preferring tetra- and octahedral or even icosahedral geometries were also suited for complex formation provided that the salen groups of the ligand molecules were mobile enough to attain the corresponding geometry. The resulting coordination polymer films are deeply colored, with the color being dependent on the metal ions involved. Films containing PSVA and copper(II), iron(III), or cerium(IV) can be oxidized electrochemically, but unfortunately, the oxidation is either partially or fully irreversible.

Acknowledgment. We thank Ruth Bruker and Prof. Meerholz for their help with the SEM studies and thickness measurements. The help of Prof. Werner Rammensee, Institut für Geologie und Mineralogie, Universität zu Köln, with the SFM study is gratefully acknowledged. The Deutsche Forschungsgemeinschaft is thanked for supporting the project financially (Project Ti 219/6-3).

LA062044C